Article

Not peer-reviewed version

Exploring the Role of CT-Based Delta-Radiomics in Unresectable Vulvar Cancer

Abdulla Alzibdeh , Bara M. Hammadeh , Mohammad Abd Al-Raheem , Rima Mheidat , Alzahra'a Al matairi , Mohamed Qamber , Hanan Almasri , Bayan Altalla' , Amal Al-Omari , Rahaf Alnajjar , Fawzi Abuhijla *

Posted Date: 5 September 2025

doi: 10.20944/preprints202509.0510.v1

Keywords: vulvar cancer; delta-radiomics; radiomics; CT simulation; gross tumor volume (GTV); prognosis and risk stratification; local control; overall survival; adaptive radiotherapy

 doi:10.20944/preprints202509.0510.v1

Article

Exploring the Role of CT-based Delta-Radiomics in Unresectable Vulvar Cancer

Abdulla Alzibdeh [1], Bara M. Hammadeh [2], Mohammad Abd Al-Raheem [1], Rima Mheidat [1], Alzahra'a Al matairi [3], Mohamed Qamber [4], Hanan Almasri [1], Bayan Al-Talla' [1], Amal Al-Omari [1], Rahaf Alnajjar [1] and Fawzi Abuhijla [1,*]

[1] King Hussein Cancer Center, Amman, Jordan,
[2] Faculty of Medicine, Al-Balqa' Applied University, Salt, Jordan,
[3] Faculty of Medicine, University of Jordan, Amman, Jordan,
[4] King Hussain Cancer Center, Amman, Jordan
* Correspondence: fhijle@khcc.jo

Abstract

Purpose: To explore the prognostic potential of gross tumor volume (GTV)–based delta-radiomic features from CT simulation scans in patients with locally advanced unresectable vulvar cancer. **Methods:** A total of 21 patients (between 2019–2024) undergoing definitive radiotherapy were included, with baseline and post–phase-I (after 25 fractions) CT simulation scans analyzed. Radiomic features (n = 107) were extracted from GTVs using PyRadiomics, and delta features were calculated as the relative change between scans. A multi-step selection pipeline (univariable Cox screening ($p < 0.10$), correlation filtering and Lasso-Cox) was applied for each endpoint: local control (LC), regional control, distant metastasis–free survival, progression-free survival, and overall survival (OS). Model discrimination was assessed via 500-iteration bootstrapped concordance index (C-index), and calibration was plotted at 24 months. **Results:** Median follow-up was 50.0 months. The 2-year LC and OS rates were 56.2% and 55.9%, respectively. Final multivariable models retained a sole texture Δ feature for LC (HR = 2.62, 95% CI = 1.05–6.52, $p = 0.039$; C-index = 0.748) and six Δ features for OS (C-index = 0.864). No features were retained for other endpoints. For LC, increased run-length non-uniformity after phase I predicted poorer control. For OS, increased texture/shape complexity predicted worse survival, whereas increased uniformity predicted better survival. **Conclusion:** CT-based delta-radiomic features, particularly shape and texture metrics, may predict LC and OS in unresectable vulvar cancer. Despite the small sample size, these findings highlight the potential for delta-radiomics as a noninvasive biomarker for risk stratification. Validation in larger cohorts and exploring potential in adaptive radiotherapy are warranted.

Keywords: vulvar cancer; delta-radiomics; radiomics; CT simulation; gross tumor volume (GTV); prognosis and risk stratification; local control; overall survival; adaptive radiotherapy

1. Introduction

Vulvar cancer is a rare but increasingly diagnosed gynecological cancer, accounting for nearly 5% of all gynecologic malignancies [1,2]. Squamous cell carcinoma accounts for 95% of cases [3]. It is considered a significant clinical challenge, especially in its advanced stages. The management of locally advanced unresectable vulvar cancer usually involves definitive chemoradiation [4]. However, outcomes remain poor, underscoring the need for improved prognostic tools [5–7].

Locoregional rather than distant failures account for most treatment relapses in vulvar cancer, carrying substantial morbidity and offer limited salvage options [8,9]. Distant metastases are uncommon and typically occur only after locoregional relapse [8]. Patients who experience locoregional or distant recurrence have markedly poorer survival rates [10].

 doi:10.20944/preprints202509.0510.v1

Radiomics, the high-throughput extraction of quantitative data from medical images, has become a valuable approach for describing tumor heterogeneity and predicting clinical outcomes. Radiomic features extraction from computed tomography (CT) images has become increasingly known as a non-invasive biomarker that have the potential to help in cancer prognostics [11,12]. CT simulation scans are routinely obtained for all radiotherapy patients and thus represent a readily available source of segmented images, with data that can help predict response to treatment, prognosis and treatment-related toxicities [13–15]. In March, 2025, Xiao et al. constructed a model combining CT-based radiomic features and clinical indices can predict overall survival (OS) in cervical cancer patients treated with intensity-modulated radiotherapy (IMRT) and concurrent chemotherapy [16].

Another extension of this work is "delta-radiomics," which assesses changes in radiomic features over the course of therapy [17]. In cervical cancer, delta-radiomics has shown promising results in predicting intermediate and high-risk pathological factors in patients receiving neoadjuvant therapy [18], and may even outperform FIGO stage and MRI-assessed maximum tumor diameter in prognostication of locally advanced cervical cancer treated with chemoradiotherapy [19].

Despite the huge advancements in the field of radiomics and delta-radiomics, the application of delta-radiomics in vulvar cancer remains underexplored. Given the ability of delta-radiomics to identify treatment-related changes and predict clinical outcomes, examining its utility in vulvar cancer could provide valuable insights. The present study aims to evaluate the prognostic potential of delta-radiomic features extracted from CT simulation images in patients with locally advanced unresectable vulvar cancer, focusing on their association with local control (LC), regional control (RC), distant metastasis-free survival (DMFS), progression-free survival (PFS), and OS.

2. Methods

2.1. Patients

In this study, we retrospectively reviewed the records of patients with histologically confirmed, locally advanced, unresectable vulvar squamous cell carcinoma treated at our institution between January 2019 and December 2024. Unresectable disease was defined as primary tumors not amenable to complete surgical excision without unacceptable morbidity, based on multidisciplinary team assessment. Inclusion criteria included: (i) availability of baseline CT simulation scans acquired before the start of definitive radiotherapy and a second CT simulation scan acquired after the first phase of treatment (25 fractions), (ii) gross tumor volume (GTV) of the primary vulvar tumor contoured by the treating radiation oncologist on both scans, and (iii) complete clinical and follow-up data for the study endpoints. Patients with incomplete imaging, inadequate ROI segmentation, or missing follow-up information were excluded. A minimum follow-up duration of 3 months was required. Demographic, clinical, and treatment-related variables were retrieved from electronic medical records, including age at diagnosis, performance status, FIGO stage, radiotherapy dose and technique, concurrent chemotherapy administration, and follow-up duration.

2.2. Treatment, CT Acquisition Parameters and Segmentation

All patients received definitive radiotherapy in two phases. Phase I consisted of 45 Gy delivered in 25 daily fractions, five fractions per week. Field of radiotherapy included the primary vulvar tumor and inguino-pelvic lymph nodes. Phase II subsequently brought the total dose to 60–66 Gy over 30–33 fractions, with a field encompassing the primary vulvar tumor, and involved lymph nodes were included to the maximum tolerable dose. Concurrent chemotherapy consisted of cisplatin at dose of 40mg/mm^2, administered weekly [20].

All patients underwent CT simulation in the supine position, with straight-leg position. As contrast-enhanced CT is not routinely used in simulation for definitive radiotherapy, all included images were acquired without contrast. Scans were acquired using Philips Brilliance Big Bore CT (85-cm bore) with a 3-mm slice thickness, axial slices, extending from at least the L2 vertebral level to

 doi:10.20944/preprints202509.0510.v1

below the perineum. Baseline CT simulation scans were obtained within two weeks prior to the start of radiotherapy, and post–phase I scans were performed after completion of 25 fractions, prior to initiating the second phase of treatment. Contouring and planning were done using the Pinnacle^3 16.2 (Philips Medical System) treatment planning system [21]. All imaging data were stored in DICOM format and retrieved from the institutional radiotherapy planning system for subsequent processing and radiomic feature extraction.

2.3. Radiomic Feature Extraction

Radiomic features were extracted from CT simulation images acquired before and after the first phase of definitive radiotherapy; first scan is before starting radiotherapy, and second scan is after 25 fractions. The pipeline was implemented in Python using open-source libraries including PyRadiomics [22], SimpleITK, pydicom, and rt_utils.

2.4. DICOM Image and RT Structure Acquisition

CT simulation data were retrieved in DICOM format. For each patient, the CT series was read using SimpleITK's ImageSeriesReader, which reconstructs the three-dimensional image volume. The resulting CT image was saved as a NIfTI file. In parallel, the corresponding RT structure set (RTSTRUCT) was accessed using pydicom. The ROI corresponding to the gross tumor volume (GTV) of the primary vulvar tumor contoured by treating radiation oncologist was then selected for feature extraction.

2.5. ROI Mask Generation

The RTSTRUCT file was combined with the CT DICOM series using the RTStructBuilder from the rt_utils package. The builder generated a binary mask. Given that the default output shape of the mask was (width, height, slices), the mask array was transposed to ensure correct spatial interpretation by SimpleITK. This transposed binary mask was then converted into a SimpleITK image and its spatial metadata was aligned with that of the CT image. The resulting ROI mask was saved in NIfTI format.

2.6. Radiomic Feature Extraction

Radiomic feature extraction was performed using PyRadiomics. The saved CT image and corresponding ROI mask were loaded as SimpleITK images. A default PyRadiomics feature extractor was instantiated, and 107 quantitative features (including first-order statistics, shape, and texture features based on gray-level co-occurrence, run-length, size-zone, and neighboring gray tone difference matrices) were extracted. This entire pipeline was repeated for both baseline and post-25-fraction CT scans for each patient, thereby enabling a delta-radiomic analysis to evaluate changes in features with respect to survival outcomes.

2.7. Calculation of Delta-Radiomics

Delta-radiomic features, or Δ features, were computed to capture the intra-treatment variation in imaging features. The formula used was:

$$Delta\ Feature = \frac{F_{post} - F_{pre}}{F_{pre}}$$

Where F_{pre} and F_{post} are the radiomic features from the baseline and post-phase-I scans, respectively.

To ensure comparability across features with different scales, a z-score normalization was applied to the Δ features (Δ features). This transformation rescales the data to have a mean of zero and a standard deviation of one.

2.8. Feature Selection for Survival Outcomes

 doi:10.20944/preprints202509.0510.v1

To select delta-radiomic features for prediction of outcomes, we first performed univariable Cox proportional-hazards regression for each Δ feature against each of the 5 endpoints (LC, RC, DMFS, PFS, and OS), retaining only those with a two-sided p-value < 0.10. Next, we computed pairwise Pearson correlations among the retained features and eliminated one member of any pair with $|r| > 0.90$, dropping the feature with the weaker univariable association. This step reduces redundant features and combat collinearity. The yielded set of Δ features was then fed into a Lasso-penalized Cox model (L1 regularization) with penalty strength λ chosen via five-fold cross-validated concordance index maximization. Δ features with non-zero coefficients at the optimal λ were deemed robust predictors. Finally, Lasso-selected Δ features were entered into an unpenalized Cox model and a bidirectional stepwise selection based on Akaike's Information Criterion (AIC) was done. The complete workflow of image processing and radiomics analysis is illustrated in Figure 1.

 doi:10.20944/preprints202509.0510.v1

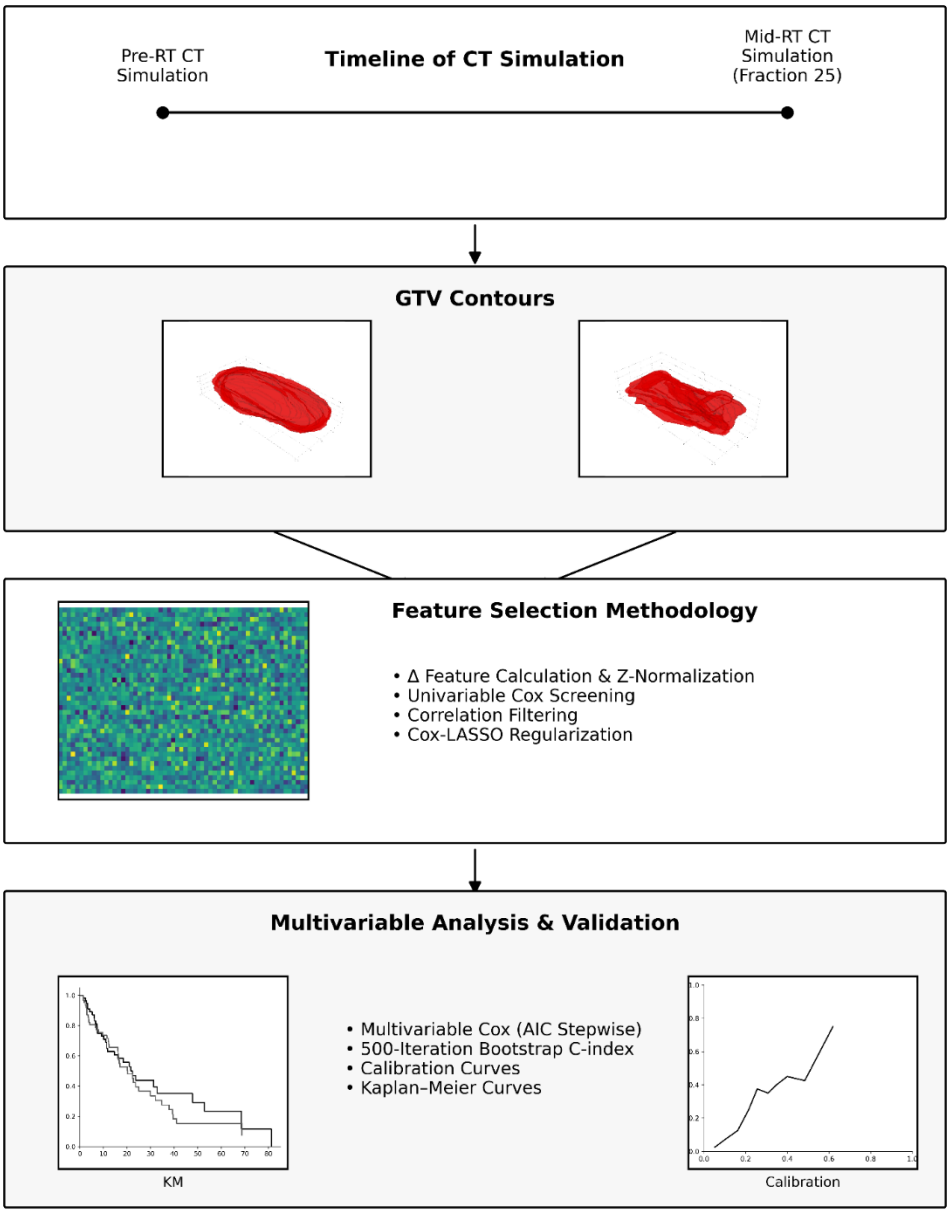

Figure 1. Radiomics analysis workflow. Radiomic features were extracted from gross tumor volume (GTV) masks delineated on pre- and mid-radiotherapy CT simulation scans. Delta features (Δ features) were calculated and Z-normalized. Feature selection was performed sequentially using univariable Cox proportional hazards screening, correlation filtering, and Cox–LASSO regularization, to identify predictors of local control (LC), regional control (RC), distant metastasis–free survival (DMFS), progression-free survival (PFS), and overall survival (OS). Several features were retained for LC and OS prediction, with no features retained for RC, DMFS, or PFS. Final models were developed using multivariable Cox regression with Akaike Information Criterion (AIC)-based stepwise selection, and their performance was evaluated using 500-iteration bootstrap concordance index (C-index) estimation, calibration curves, and Kaplan–Meier survival analysis.

 doi:10.20944/preprints202509.0510.v1

2.9. Statistical Analysis

Patients' characteristics were reported as medians, interquartile ranges (IQR), counts and percentages. Median follow-up was calculated using reverse Kaplan-Meier method. Rates of each survival endpoint of LC, RC, DMFS, PFS and OS, were reported as median, 2-year and 4-year rates. Results of significant univariate Cox proportional hazards regression were reported in the supplementary material. For multivariable analysis, proportional-hazards assumptions were assessed using Schoenfeld residuals (all global and covariate-specific tests should be $p > 0.05$). For covariates showing evidence of violation, time-varying effects were modeled by adding covariate–log(time) interaction terms, and the stepwise selection procedure was repeated with hierarchical retention of main effects. Multicollinearity was assessed by calculating variance inflation factors (all VIFs should be < 5). Results of the final cox model after feature selection were reported in terms of hazard ratios (HR) and CI for each Δ feature, along with the 500-iteration bootstrapped C-index. Calibration plots were provided as supplementary material. A p-value < 0.05 was deemed significant. All statistical analyses were performed using Python version 3.11.13.

3. Results

3.1. Patient Characteristics

Twenty-one patients with locally advanced unresectable vulvar cancer were included. Table 1 shows patients' characteristics and treatment specifics. The median age at diagnosis was 57.0 years (range: 37–79 years; IQR: 17.0). All patients were treated with definitive radiotherapy. Radiotherapy was planned via volumetric modulated arc therapy (VMAT) in all patients. The total vulvar radiotherapy dose had a median of 65.0 Gy (IQR: 2.6), while the median dose of first phase of radiotherapy in Gy was 45.0 (IQR: 5.4). Only one patient did not receive concurrent chemotherapy with radiotherapy.

Table 1. Patients and Disease Characteristics and Treatment Specifics (n = 21).

Variable	**Median**	**IQR**	
Age at diagnosis (years)	57	17	
Total vulvar dose (Gy)	65	2.6	
External-beam Radiotherapy dose in Gy	45	5.4	
External-beam Radiotherapy number of fractions	25	3	
Nodal dose (Gy)	63	12	
EBRT Time (days)	54	10	
Chemotherapy cycles	5	1	
Variable	**Category**	**Count**	**Percentage (%)**
Grade	1	1	4.8
	2	15	71.4
	3	4	19
	Missing	1	4.8
HPV Categories	Not associated	12	57.1
	HPV-associated	7	33.3
	Missing	2	9.5
FIGO Stage	II	1	4.8
	IIIA	1	4.8
	IIIB	7	33.3
	IIIC	1	4.8
	IVA	2	9.5
	IVB	6	28.6

 doi:10.20944/preprints202509.0510.v1

	Missing	3	14.3
Concurrent Chemotherapy	Yes	20	95.2
	No	1	4.8

3.2. Treatment Outcomes

After a median follow-up of 50.0 months (IQR 10.7–59.0), median LC was not reached, with the 2-year rate of 56.2% (95% CI 29.0–76.5). RC median was also not reached, with 2-year rate being 65.7% (95% CI 33.6–85.1). Median DMFS was 20.0 months (95% CI 11.3–71.0), and the 2-year rate was 44.3% (95% CI 19.3–66.8). Median PFS was 10.0 months (95% CI 8.0–67.0), and the 2-year PFS rate was 36.1% (95% CI 13.7–59.3). Notably, most or all of the events counted by these four endpoints occurred before 2 years, as evident in Table 2. Median OS was 28.0 months (95% CI 16.2–71.0), and the 2-year was 55.9% (95% CI 28.4–76.4). Survival curves are illustrated in Figure 2.

Table 2. Treatment outcomes.

Endpoint	Events (n)	Total (n)	Event rate (%)	Events ≤24 months (n)	≤24 months (%)
Local Control	8	21	38.1	7	87.5
Regional Control	5	21	23.8	5	100.0
Distant Metastasis–Free	9	21	42.9	9	100.0
Progression–Free	12	21	57.1	11	91.7
Overall Survival	9	21	42.9	7	77.8

 doi:10.20944/preprints202509.0510.v1

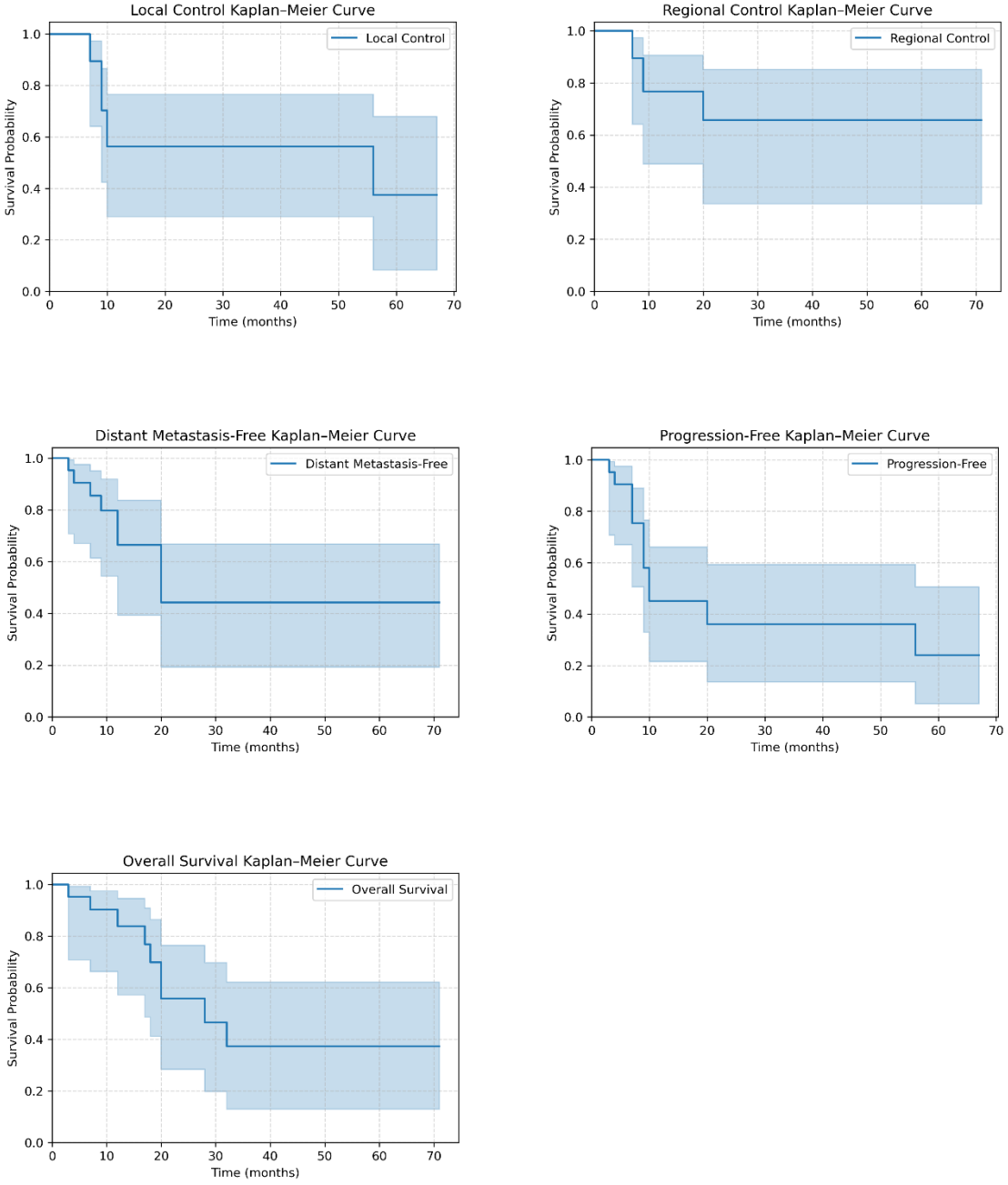

Figure 2. Kaplan–Meier curves for local control (LC), regional control (RC), distant metastasis–free survival (DMFS), progression–free survival (PFS), and overall survival (OS) in the study cohort.

3.3. Univariable Analyses and Feature Selection

On univariable cox regression, several significant Δ features were yielded for each endpoint, and those with a p value of < 0.1 are reported in Supplementary Table 1, along with Kaplan-Meier curves for those with a p value of < 0.5 (Supplementary figures 1-4; none had a p value of < 0.5 for RC).

All Δ features with a p value of < 0.1 were included in the pairwise Pearson correlations (Supplementary Table 2). After excluding redundant Δ features, a Lasso-penalized Cox model was run for each endpoint. At this step, only LC and OS retained any Δ features; no features survived selection for RC, DMFS, or PFS. Selected Δ features that were included in the multivariable analyses

 doi:10.20944/preprints202509.0510.v1

are illustrated in Table 3. Supplementary Table 3 shows the temporal changes in Δ features retained in final models.

Table 3. Feature selection results for study endpoints.

Endpoint	Selected Δ features
LC	GLCM Inverse Difference Moment (IDM)
	GLRLM Run Length Non-Uniformity Normalized (RLNU_norm)
	GLRLM Run Percentage (RP)
	First-order Entropy
	GLCM Difference Entropy (DiffEnt)
	GLCM Cluster Prominence (ClusProm)
RC	*none retained*
DMFS	*none retained*
PFS	*none retained*
OS	GLCM Difference Average (DiffAvg)
	Shape Surface-Volume Ratio (SVR)
	GLCM Difference Variance (DiffVar)
	GLDM Large Dependence Low Gray-Level Emphasis (LDLGLE)
	GLSZM Size Zone Non-Uniformity (SZNU)
	GLSZM Gray-Level Non-Uniformity Normalized (GLNU_norm)
	GLSZM Zone Entropy (ZoneEnt)
	GLSZM Gray-Level Variance (GLVar)
	First-order Energy

LC, Local Control; RC, Regional Control; DMFS, Distant Metastasis-Free Survival; PFS, Progression-Free Survival; OS, Overall Survival; GLCM, Gray-Level Co-occurrence Matrix; GLRLM, Gray-Level Run-Length Matrix; GLSZM, Gray-Level Size-Zone Matrix; GLDM, Gray-Level Dependence Matrix; First-order, features derived from the voxel intensity histogram without spatial context.

3.4. Multivariable Analyses and Internal Validation

After AIC-based bidirectional stepwise selection, the final multivariable Cox model for LC only retained the Δ RLNU_norm with a coefficient of 0.962 (HR: 2.62, 95% CI: 1.05–6.52; p = 0.039, Table 4). This translates into more than doubling of the hazard of local recurrence for each one–standard-deviation increase in Δ RLNU_norm. the 500-iteration bootstrap yielded a mean C-index of 0.748 (95% CI 0.506–0.987, Figure 3).

Table 4. Multivariable Cox model with AIC-based bidirectional stepwise selection for LC and OS.

Multivariable Cox model for LC (retaining one variable)				
Δ Feature	**Coef**	**HR**	**95% CI**	**p-value**
GLRLM Run-Length Non-Uniformity Normalized (**RLNU_norm**)	0.9625	2.618	[1.05, 6.52]	0.0388
Multivariable Cox model for OS (time-varying)				
Feature	**Coef**	**HR**	**95% CI**	**p-value**
GLCM Difference Average (DiffAvg)	–9.0097	0.00012	[3×10^{-8}, 0.48]	0.0327
Shape Surface-Volume Ratio (SVR)	5.7666	319.45	[1.74, 5.9×10^{4}]	0.0302
GLCM Difference Variance (DiffVar)	5.7931	328.02	[1.33, 8.1×10^{4}]	0.0393
GLDM Large Dependence Low Gray-Level Emphasis (LDLGLE)	–8.3732	0.00023	[1×10^{-8}, 5.28]	0.1021
GLSZM Gray-Level Non-Uniformity Normalized (GLNU_norm)	–9.2533	0.00010	[3×10^{-8}, 0.33]	0.0259

 doi:10.20944/preprints202509.0510.v1

First-order Energy	–1.6158	0.1987	[0.03, 1.22]	0.0807

LC, Local Control; OS, Overall Survival; GLCM, Gray-Level Co-occurrence Matrix; GLRLM, Gray-Level Run-Length Matrix; GLSZM, Gray-Level Size-Zone Matrix; GLDM, Gray-Level Dependence Matrix; First-order, features derived from the voxel intensity histogram without spatial context.

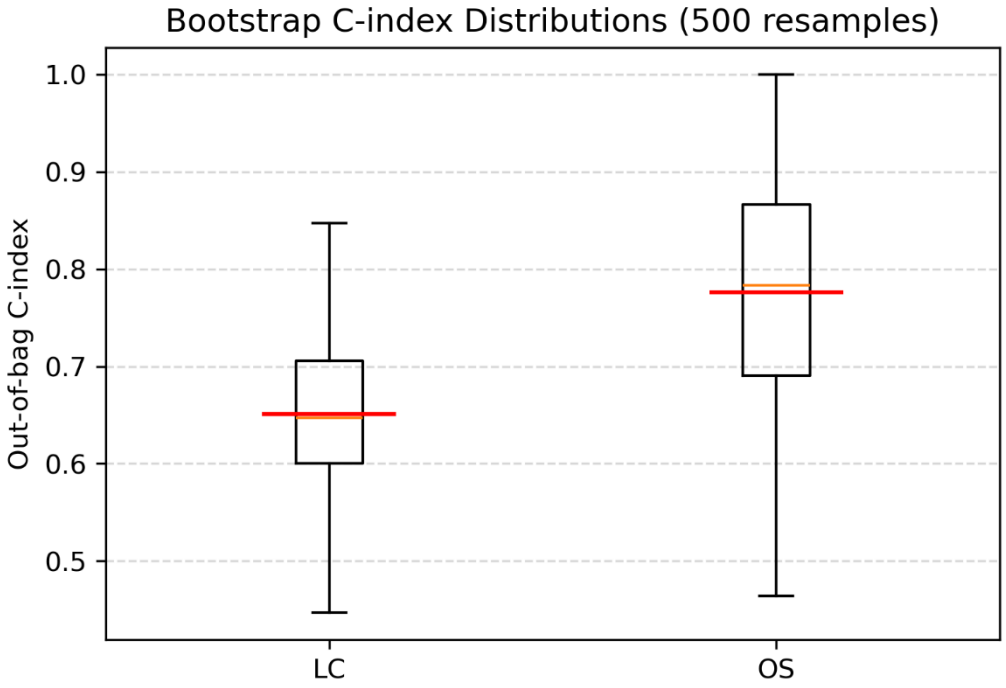

Figure 3. Bootstrapped concordance index (C-index) for the final multivariable Cox models predicting local control (LC) and overall survival (OS). The LC model retained only ΔRLNU_norm (C-index = 0.751), while the OS model retained six Δ features (C-index = 0.896).

For OS, time-varying effects were incorporated in the final multivariable Cox proportional hazards model to address violations of the proportional hazards assumption identified in initial testing. Bidirectional stepwise selection retained six Δ features (Table 4). Among these, Δ DiffAvg, Δ SVR, Δ DiffVar, and Δ GLNU_norm were statistically significant ($p < 0.05$); greater increases in texture or contrast (DiffVar, SVR) seem to portend worse survival, whereas larger increases in uniformity metrics (DiffAvg, GLNU_norm) predicter better survival. All retained variables satisfied the proportional hazards assumption in the final model. The bootstrap-corrected C-index for the OS model was 0.864 (95% CI 0.633–0.973, Figure 3). Calibration plots are illustrated in supplementary Figure 5.

4. Discussion

This hypothesis-generating study is the first to provide proof-of-concept that CT GTV-based delta-radiomics may serve as a non-invasive biomarker in patients with locally advanced unresectable vulvar cancer. Using a rigorous feature selection pipeline, including univariable Cox screening, correlation filtering, Cox-Lasso regularization, and AIC-based selection, several features were nominated to predict LC and OS, with no features retained for RC, DMFS and PFS. This likely reflects the source of the features, the GTV, and highlights the fact that predictors of the more common failure pattern, local failure, are likely to predict worse OS in our group of patients.

Such dimensionality reduction is of paramount importance in radiomics studies, where multiple testing can lead to falsely significant findings [23]. Although multiple significant Δ features on univariable cox analyses were yielded (Supplementary Table 1), none were retained after our multi-step feature selection process, as described in results.

 doi:10.20944/preprints202509.0510.v1

Our multivariable Cox model for LC identified one significant feature, RLNU_norm. This texture-based metric captures how uniform the run lengths (i.e., sequences of the same gray level) are in the GTV [22]. Each one unit increase in the RLNU_norm is associated with a 2.6-fold higher hazard of local recurrence (Table 4); the more run-length heterogeneity the tumor becomes after first phase of radiotherapy, the worse its LC is expected to be. For OS, the model retained six Δ features, of which four were significant, indicating that increased uniformity (e.g., in Δ GLNU_norm and Δ DiffAvg) predicted better survival, while increased heterogeneity or complexity (Δ SVR and Δ DiffVar) predicted worse outcomes.

Table 4. Multivariable Cox model with AIC-based bidirectional stepwise selection for LC and OS.

Multivariable Cox model for LC (retaining one variable)				
Δ Feature	**Coef**	**HR**	**95% CI**	**p-value**
GLRLM Run-Length Non-Uniformity Normalized (**RLNU_norm**)	0.9625	2.618	[1.05, 6.52]	0.0388
Multivariable Cox model for OS (time-varying)				
Feature	Coef	HR	95% CI	p-value
GLCM Difference Average (DiffAvg)	–9.0097	0.00012	[3×10^{-8}, 0.48]	0.0327
Shape Surface-Volume Ratio (SVR)	5.7666	319.45	[1.74, 5.9×10^{4}]	0.0302
GLCM Difference Variance (DiffVar)	5.7931	328.02	[1.33, 8.1×10^{4}]	0.0393
GLDM Large Dependence Low Gray-Level Emphasis (LDLGLE)	–8.3732	0.00023	[1×10^{-8}, 5.28]	0.1021
GLSZM Gray-Level Non-Uniformity Normalized (GLNU_norm)	–9.2533	0.00010	[3×10^{-8}, 0.33]	0.0259
First-order Energy	–1.6158	0.1987	[0.03, 1.22]	0.0807

LC, Local Control; OS, Overall Survival; GLCM, Gray-Level Co-occurrence Matrix; GLRLM, Gray-Level Run-Length Matrix; GLSZM, Gray-Level Size-Zone Matrix; GLDM, Gray-Level Dependence Matrix; First-order, features derived from the voxel intensity histogram without spatial context.

Our multivariable model for OS had a 500-iteration bootstrap C-index of 0.87 (95 % CI 0.61–0.97), indicating a strong discrimination, despite the limited sample size and only 9 captured events. Such findings suggest a promising role of radiomics and delta-radiomics for vulvar cancer prognostication and risk-stratification.

Our findings suggest that residual tumors exhibiting more irregular shapes and higher texture heterogeneity during radiotherapy may reflect treatment resistance and portend worse outcomes. Increasing SVR, a shape feature, reflects the increasing tumor surface complexity relative to volume during treatment. This change can be attributed to the development of infiltrative growth patterns, spiculated borders resulting from radiation-induced fibrosis (or the persistence of aggressive tumor clones), and a necrotic core that leaves uneven tumor surfaces [24].

It has been shown that in carcinoma, metastatic potential is acquired through early molecular changes such as epithelial-to-mesenchymal transformation, orchestrated by the tumor microenvironment and stromal interactions [25]. Whether this heterogeneity in radiomic features reflects the molecular diversity of tumor clones remains a question for future translational studies. Another mystery to be unfolded is whether using subregional segmentation instead of whole GTV as the region of interest to extract radiomic features would capture the well-known intra-tumoral heterogeneity, which may help sharpen the performance of radiomics [26].

We chose to focus on unresectable vulvar cancer because prognostic markers are less well established in this setting. In such cases, tumor-derived radiomic features may represent an important source of prognostic information, whereas in post-surgical scenarios, numerous other determinants, such as pathological findings, margin status, and treatment-related factors, are readily available and have been validated to play a substantial role in outcome prediction [27].

Prior delta-radiomic studies in cervical cancer have demonstrated prognostic value for response to treatment and survival outcomes [16,18,19]. However, vulvar cancer has been underrepresented

 doi:10.20944/preprints202509.0510.v1

in radiomics research, with a single study that used ^{18}F-FDG PET/CT-based radiomics to correlate with tumor biology and predict prognosis. Our study addresses this gap and suggests that even in rare cancers, quantitative imaging biomarkers can be developed using standardized pipelines. Moreover, our findings align with prior evidence suggesting that local control, more than distant failure, remains the main challenge in locally advanced vulvar cancer, and potentially determines outcomes in vulvar cancer [7,10,28], thus justifying the focus on GTV-derived features.

CT simulation scans are routinely obtained in radiotherapy planning, and our reliance on these widely available images enhances clinical applicability. Such scans are usually contoured by experienced radiation oncologists according to established contouring guidelines [29]. While MRI and PET/CT may offer more detailed soft-tissue characterization or metabolic data [19,30], their availability, cost, and variability in segmentation limit generalizability. A model based solely on Δ features from segmented CT scans could be integrated into existing workflows with minimal disruption, across different socioeconomic settings. Moreover, results on delta-radiomic features raise the potential for adaptive radiotherapy, where patients with unfavorable delta-radiomic profiles could be flagged early for treatment modifications [31,32]. In fact, prior clinical observations in vulvar cancer indicate that more than half of patients require adaptive replanning during definitive radiotherapy, particularly those with large baseline tumor volumes [33].

Limitations

Our study has several limitations. First, its single-center, retrospective design, small sample size and the lack of external validation reduce its statistical power, and increase the risk of overfitting, all of which may limit the generalizability and reproducibility of the findings. Also, the small sample size hindered the calculation of distant control analysis, as some studies report this event in as few as 5.1% of the cases only [8]. Nonetheless, our limited sample size reflects the rarity of unresectable vulvar cancer. Such obstacle was mitigated by using a multi-step feature selection pipeline with internal bootstrapping and calibration to ensure robustness and reduce overfitting. Accordingly, our results should be interpreted as exploratory, but they provide a rationale for larger multi-institutional validation. Future multi-institutional collaboration will be essential for external validation.

Another limitation is the potential subjectivity in ROI contouring, which may affect reproducibility. This reflects the complexity of available consensuses for vulvar cancer contouring, which are difficult to be prescriptive for every patient scenario, especially in the locally advanced unresectable setting [34,35].

FIGO staging was not included in the final model to avoid overloading the analysis with predictors given the small sample size. Moreover, staging variability was minimal in our cohort, as nearly all patients had stage III–IV disease.

Although contrast-enhanced CT could potentially enhance the prognostic performance of radiomic models, it is not routinely used in simulation for vulvar cancer radiotherapy. Also, feature extraction from contrast-enhanced CT scans introduces potential variability and may not be reproducible across institutions. Using non-enhanced images is more translatable to standard clinical workflows and is safer in patients with kidney impairment.

5. Conclusions

In this study, we demonstrate that CT-based delta-radiomic features, particularly shape and texture metrics, hold a potential prognostic value in locally advanced unresectable vulvar cancer. These features capture intra-treatment changes in tumor morphology and heterogeneity that correlate with LC and OS, potentially offering earlier and more objective risk stratification than conventional methods. While our single-center experience provides foundational evidence for delta-radiomics in this rare malignancy, larger multi-institutional studies are needed to validate these findings. Such noninvasive biomarkers provide hope to guide personalized therapeutic strategies. Future work should integrate radiomics with histopathological and genomic data to elucidate the biological underpinnings of these imaging phenotypes.

 doi:10.20944/preprints202509.0510.v1

Supplementary Materials: The supporting information can be downloaded at the website of this paper posted on Preprints.org.

Acknowledgments: We would like to thank Mohammad Atari for his expert guidance and support with statistical methodology and analyses.

Ethics approval: This retrospective study data was approved by the Institutional Review Board (IRB) (25 KHCC 028) on 3 September 2025.

References

1. Siegel RL, Kratzer TB, Giaquinto AN, Sung H, Jemal A. Cancer statistics, 2025. CA Cancer J Clin [Internet]. 2025 Jan 1 [cited 2025 Aug 7];75(1):10–45. Available from: /doi/pdf/10.3322/caac.21871
2. Buttmann-Schweiger N, Klug SJ, Luyten A, Holleczek B, Heitz F, Du Bois A, et al. Incidence Patterns and Temporal Trends of Invasive Nonmelanotic Vulvar Tumors in Germany 1999-2011. A Population-Based Cancer Registry Analysis. PLoS One [Internet]. 2015 May 28 [cited 2025 Aug 7];10(5):e0128073. Available from: https://journals.plos.org/plosone/article?id=10.1371/journal.pone.0128073
3. Alkatout I, Schubert M, Garbrecht N, Weigel MT, Jonat W, Mundhenke C, et al. Vulvar cancer: Epidemiology, clinical presentation, and management options. Int J Womens Health [Internet]. 2015 Mar 20 [cited 2025 Aug 7];7:305–13. Available from: https://pubmed.ncbi.nlm.nih.gov/25848321/
4. Abu-Rustum NR, Yashar CM, Arend R, Barber E, Bradley K, Brooks R, et al. Vulvar Cancer, Version 3.2024. JNCCN J Natl Compr Cancer Netw [Internet]. 2024 Mar 1 [cited 2025 Aug 7];22(2):117–35. Available from: https://pubmed.ncbi.nlm.nih.gov/38503056/
5. Rao YJ, Chin RI, Hui C, Mutch DG, Powell MA, Schwarz JK, et al. Improved survival with definitive chemoradiation compared to definitive radiation alone in squamous cell carcinoma of the vulva: A review of the National Cancer Database. Gynecol Oncol [Internet]. 2017 Sep 1 [cited 2025 Aug 7];146(3):572–9. Available from: https://pubmed.ncbi.nlm.nih.gov/28662775/
6. Macchia G, Lancellotta V, Ferioli M, Casà C, Pezzulla D, Pappalardi B, et al. Definitive chemoradiation in vulvar squamous cell carcinoma: outcome and toxicity from an observational multicenter Italian study on vulvar cancer (OLDLADY 1.1). Radiol Med [Internet]. 2023 Jan 1 [cited 2025 Aug 7];129(1):152. Available from: https://pmc.ncbi.nlm.nih.gov/articles/PMC10808465/
7. Kim Y, Kim JY, Kim JY, Lee NK, Kim JH, Kim YB, et al. Treatment outcomes of curative radiotherapy in patients with vulvar cancer: results of the retrospective KROG 1203 study. Radiat Oncol J [Internet]. 2015 Sep 1 [cited 2025 Aug 7];33(3):198. Available from: https://pmc.ncbi.nlm.nih.gov/articles/PMC4607573/
8. Prieske K, Haeringer N, Grimm D, Trillsch F, Eulenburg C, Burandt E, et al. Patterns of distant metastases in vulvar cancer. Gynecol Oncol [Internet]. 2016 Sep 1 [cited 2025 Aug 7];142(3):427–34. Available from: https://www.gynecologiconcology-online.net/action/showFullText?pii=S0090825816308782
9. Salom EM, Penalver M. Recurrent vulvar cancer. Curr Treat Options Oncol [Internet]. 2002 Apr 1 [cited 2025 Aug 7];3(2):143–53. Available from: https://pubmed.ncbi.nlm.nih.gov/12057077/
10. Zach D, Åvall-Lundqvist E, Falconer H, Hellman K, Johansson H, Flöter Rådestad A. Patterns of recurrence and survival in vulvar cancer: A nationwide population-based study. Gynecol Oncol [Internet]. 2021 Jun 1 [cited 2025 Aug 7];161(3):748–54. Available from: https://pubmed.ncbi.nlm.nih.gov/33736857/
11. Aerts HJWL, Velazquez ER, Leijenaar RTH, Parmar C, Grossmann P, Cavalho S, et al. Decoding tumour phenotype by noninvasive imaging using a quantitative radiomics approach. Nat Commun [Internet]. 2014 Jun 3 [cited 2025 Aug 7];5. Available from: https://pubmed.ncbi.nlm.nih.gov/24892406/
12. Manganaro L, Nicolino GM, Dolciami M, Martorana F, Stathis A, Colombo I, et al. Radiomics in cervical and endometrial cancer. Br J Radiol [Internet]. 2021 Sep 1 [cited 2025 Aug 7];94(1125). Available from: https://pubmed.ncbi.nlm.nih.gov/34233456/
13. Zhou C, Hou L, Tang X, Liu C, Meng Y, Jia H, et al. CT-based radiomics nomogram may predict who can benefit from adaptive radiotherapy in patients with local advanced-NSCLC patients. Radiother Oncol [Internet]. 2023 Jun 1 [cited 2025 Aug 7];183:109637. Available from: https://www.thegreenjournal.com/action/showFullText?pii=S0167814023001755

 doi:10.20944/preprints202509.0510.v1

14. Kasai A, Miyoshi J, Sato Y, Okamoto K, Miyamoto H, Kawanaka T, et al. A novel CT-based radiomics model for predicting response and prognosis of chemoradiotherapy in esophageal squamous cell carcinoma. Sci Reports 2024 141 [Internet]. 2024 Jan 23 [cited 2025 Aug 7];14(1):1–10. Available from: https://www.nature.com/articles/s41598-024-52418-4
15. Nafchi ER, Fadavi P, Amiri S, Cheraghi S, Garousi M, Nabavi M, et al. Radiomics model based on computed tomography images for prediction of radiation-induced optic neuropathy following radiotherapy of brain and head and neck tumors. Heliyon [Internet]. 2025 Jan 15 [cited 2025 Aug 7];11(1):e41409. Available from: https://www.sciencedirect.com/science/article/pii/S2405844024174403
16. Xiao L, Wang Y, Shi X, Pang H, Li Y. Computed tomography–based radiomics modeling to predict patient overall survival in cervical cancer with intensity-modulated radiotherapy combined with concurrent chemotherapy. J Int Med Res [Internet]. 2025 Mar 1 [cited 2025 Aug 7];53(3):03000605251325996. Available from: https://pmc.ncbi.nlm.nih.gov/articles/PMC11938878/
17. Shur JD, Doran SJ, Kumar S, Ap Dafydd D, Downey K, O'connor JPB, et al. Radiomics in oncology: A practical guide. Radiographics [Internet]. 2021 Oct 1 [cited 2025 Aug 7];41(6):1717–32. Available from: https://pubmed.ncbi.nlm.nih.gov/34597235/
18. Wu RR, Zhou YM, Xie XY, Chen JY, Quan KR, Wei YT, et al. Delta radiomics analysis for prediction of intermediary- and high-risk factors for patients with locally advanced cervical cancer receiving neoadjuvant therapy. Sci Rep [Internet]. 2023 Dec 1 [cited 2025 Aug 7];13(1):1–8. Available from: https://www.nature.com/articles/s41598-023-46621-y
19. Wagner-Larsen KS, Lura N, Gulati A, Ryste S, Hodneland E, Fasmer KE, et al. MRI delta radiomics during chemoradiotherapy for prognostication in locally advanced cervical cancer. BMC Cancer [Internet]. 2025 Dec 1 [cited 2025 Aug 7];25(1):1–15. Available from: https://bmccancer.biomedcentral.com/articles/10.1186/s12885-025-13509-1
20. Reade CJ, Eiriksson LR, Mackay H. Systemic therapy in squamous cell carcinoma of the vulva: Current status and future directions. Gynecol Oncol [Internet]. 2014 [cited 2025 Aug 9];132(3):780–9. Available from: https://pubmed.ncbi.nlm.nih.gov/24296343/
21. Xia P, Murray E. 3D treatment planning system—Pinnacle system. Med Dosim [Internet]. 2018 Jun 1 [cited 2025 Aug 8];43(2):118–28. Available from: https://pubmed.ncbi.nlm.nih.gov/29580933/
22. Van Griethuysen JJM, Fedorov A, Parmar C, Hosny A, Aucoin N, Narayan V, et al. Computational radiomics system to decode the radiographic phenotype. Cancer Res [Internet]. 2017 Nov 1 [cited 2025 Aug 7];77(21):e104–7. Available from: https://pubmed.ncbi.nlm.nih.gov/29092951/
23. Limkin EJ, Sun R, Dercle L, Zacharaki EI, Robert C, Reuzé S, et al. Promises and challenges for the implementation of computational medical imaging (radiomics) in oncology. Ann Oncol [Internet]. 2017 Jun 1 [cited 2025 Aug 8];28(6):1191–206. Available from: https://pubmed.ncbi.nlm.nih.gov/28168275/
24. Vallières M, Kay-Rivest E, Perrin LJ, Liem X, Furstoss C, Aerts HJWL, et al. Radiomics strategies for risk assessment of tumour failure in head-and-neck cancer. Sci Reports 2017 71 [Internet]. 2017 Aug 31 [cited 2025 Aug 8];7(1):1–14. Available from: https://www.nature.com/articles/s41598-017-10371-5
25. Atiya HI, Gorecki G, Garcia GL, Frisbie LG, Baruwal R, Coffman L. Stromal-Modulated Epithelial-to-Mesenchymal Transition in Cancer Cells. Biomol 2023, Vol 13, Page 1604 [Internet]. 2023 Nov 1 [cited 2025 Aug 8];13(11):1604. Available from: https://www.mdpi.com/2218-273X/13/11/1604/htm
26. Zhang L, Wang Y, Peng Z, Weng Y, Fang Z, Xiao F, et al. The progress of multimodal imaging combination and subregion based radiomics research of cancers. Int J Biol Sci [Internet]. 2022 [cited 2025 Aug 8];18(8):3458–69. Available from: https://pubmed.ncbi.nlm.nih.gov/35637947/
27. Nooij LS, Brand FAM, Gaarenstroom KN, Creutzberg CL, de Hullu JA, van Poelgeest MIE. Risk factors and treatment for recurrent vulvar squamous cell carcinoma. Crit Rev Oncol Hematol [Internet]. 2016 Oct 1 [cited 2025 Aug 8];106:1–13. Available from: https://www.sciencedirect.com/science/article/pii/S1040842816301639
28. Woelber L, Eulenburg C, Kosse J, Neuser P, Heiss C, Hantschmann P, et al. Predicting the course of disease in recurrent vulvar cancer – A subset analysis of the AGO-CaRE-1 study. Gynecol Oncol [Internet]. 2019 Sep 1 [cited 2025 Aug 8];154(3):571–6. Available from: https://www.sciencedirect.com/science/article/abs/pii/S0090825819313952

 doi:10.20944/preprints202509.0510.v1

29. Gaffney DK, King B, Viswanathan AN, Barkati M, Beriwal S, Eifel P, et al. Consensus recommendations for radiation therapy contouring and treatment of vulvar carcinoma. Int J Radiat Oncol Biol Phys [Internet]. 2016 Jul 15 [cited 2025 Aug 8];95(4):1191–200. Available from: https://pubmed.ncbi.nlm.nih.gov/27130794/
30. Collarino A, Garganese G, Fragomeni SM, Pereira Arias-Bouda LM, Ieria FP, Boellaard R, et al. Radiomics in Vulvar Cancer: First Clinical Experience Using 18F-FDG PET/CT Images. J Nucl Med [Internet]. 2019 Feb 1 [cited 2025 Aug 8];60(2):199. Available from: https://pmc.ncbi.nlm.nih.gov/articles/PMC8833861/
31. Ger RB, Wei L, Naqa I El, Wang J. The Promise and Future of Radiomics for Personalized Radiotherapy Dosing and Adaptation. Semin Radiat Oncol [Internet]. 2023 Jul 1 [cited 2025 Aug 8];33(3):252. Available from: https://pmc.ncbi.nlm.nih.gov/articles/PMC11214660/
32. Tanaka S, Kadoya N, Sugai Y, Umeda M, Ishizawa M, Katsuta Y, et al. A deep learning-based radiomics approach to predict head and neck tumor regression for adaptive radiotherapy. Sci Rep [Internet]. 2022 Dec 1 [cited 2025 Aug 8];12(1):1–13. Available from: https://www.nature.com/articles/s41598-022-12170-z
33. Abuhijla F, Salah S, Al-Hussaini M, Mohamed I, Jaradat I, Dayyat A, et al. Factors influencing the use of adaptive radiation therapy in vulvar carcinoma. Reports Pract Oncol Radiother [Internet]. 2020 Sep 1 [cited 2025 Aug 9];25(5):709. Available from: https://pmc.ncbi.nlm.nih.gov/articles/PMC7358621/
34. Gaffney DK, King B, Viswanathan AN, Barkati M, Beriwal S, Eifel P, et al. No Title. 2016 Jul 15 [cited 2025 Aug 8];95(4). Available from: https://pubmed.ncbi.nlm.nih.gov/27130794/
35. Oonk MHM, Planchamp F, Baldwin P, Mahner S, Mirza MR, Fischerová D, et al. European Society of Gynaecological Oncology Guidelines for the Management of Patients with Vulvar Cancer - Update 2023. Int J Gynecol Cancer [Internet]. 2023 Jul 1 [cited 2025 Aug 29];33(7):1023–43. Available from: https://www.international-journal-of-gynecological-cancer.com/action/showFullText?pii=S1048891X24016323